Shape Analysis and Classification using Landmarks: Polygonal Wavelet Transform

Celina Maki Takemura [1] and **Roberto Marcondes Cesar Jr.** [2]

Abstract. Shape analysis has played a central role in many problems in vision and perception, being an active multidisciplinary research field. In this context, this paper introduces a new shape analysis approach using the well known wavelet transform and exploring shape representation by landmarks. This work shows how to obtain a time signal from the landmarks representation, which undergoes the wavelet transform, as well as a useful geometrical interpretation using two special mother wavelets, i.e. the first and the second derivatives of the gaussian. Successful experimental results obtained from real data are also discussed.

1 INTRODUCTION

Many problems in computer vision can be reduced to analyzing shapes in images, finding important applications in various disciplines such as biology and medicine e.g. for evolution studies [4, 6, 5, 10, 18]; and visual arts, security and Internet, when multimedia documents are used [9, 3]. In fact, shape analysis has played a central role in perception and signal understanding [13]. This paper introduces a method for shape analysis based on landmarks and the wavelet transform. Although the present paper only deals with 2D data, it is argued that the technique can be straightforwardly generalized to include 3D shapes.

There are different methods for suitably representing shapes for their subsequent analysis. The computer vision community has mainly followed two approaches, namely contour-based and region-based [9, 14, 16]. Among the multitude of techniques for analyzing shapes based on such representations, it is worth emphasizing the key role played by signal processing methods, such as Fourier and wavelets, which have proven to be among the most successful and widely explored ones [17, 12]. In particular, the wavelet transform has been successfully applied in many problems in signal and image processing, such as analysis of singularities [2], image fusion [7] and shape analysis [1]. In fact, the wavelet transform has been used as a tool for contour-based shape analysis that has proven to be useful due to its nice mathematical properties such as unicity, invariance and covariance to geometrical transformations and time-frequency localization.

On the other hand, the analysis of forms in natural sciences has evolved as an important discipline from the classical work of D'Arcy Thompson [20] known as morphometry that intensively explores geometrical and statistical information from shapes[6, 19, 10]. The latter makes extensive use of landmarks representation of shapes, allowing the comparison between shapes based on corresponding landmarks that are called *homologous* [5]. Landmarks are special points located in key regions of the shape of interest. It is important to note that landmarks data consists in one of the main approaches for analyzing and comparing forms in many areas such as biology, geology, anthropology and dentistry, to name but a few [12]. Nevertheless, few works have explored the analysis of landmarks-based shapes using differential and multiscale measures, which have already shown to surpass monoscale techniques in many situations.

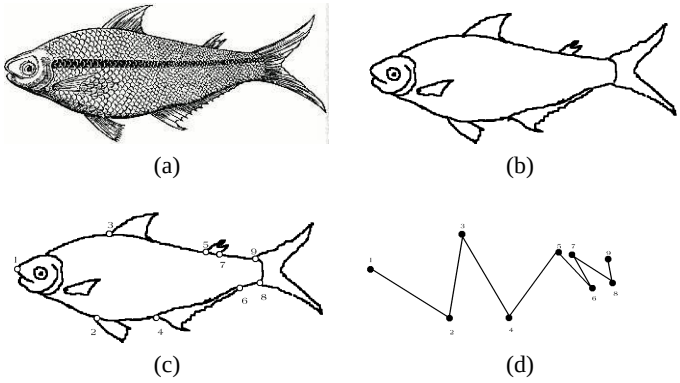

Figure 1. (a) Original image; (b) Shape contours; (c) Landmarks; (d) Shape polygonal representation. (The Piabucu fish in (a) has been reprinted from "História Natural do Brasil", [15])

Table 1. Landmarks (Inhaled in [8])

1	anterior tip of the snout on the upper jaw
2	origin of pelvic fin
3	origin of spinous dorsal fin
4	origin of anal fin
5	origin of soft dorsal fin
6	insertion of anal fin
7	insertion of 2nd dorsal fin
8	insertion of 1st ventral caudal fin ray
9	insertion of 1st dorsal caudal fin ray

This work presents a new technique to analyze landmarks data exploring the useful wavelet transform capabilities and geometrical interpretation (in the case of derivatives-of-gaussian mother wavelets). This work is organized as follows. Section 2 shows how complex-valued signals, required as input for the wavelet transform, can be obtained from the landmarks. The wavelet transform of the thus ob-

[1] Instituto de Matemáticae Estatística, Universidade de São Paulo, email: maki@ime.usp.br
[2] Instituto de Matemática e Estatísica, Universidade de São Paulo, email: cesar@ime.usp.br

tained landmarks signal is discussed in Section 3. Section 4 presents some successful results using real data. Finally, our concluding remarks are presented in Section 5.

2 FROM LANDMARKS TO SIGNALS

In general, computational shape analysis starts with an object of interest represented in a color or gray-level image as initial data. Such an image is often transformed to a suitable data structure for shape analysis, such as a contour representation of the object. In these cases, it is possible to apply procedures that transform the original image in a binary one, and then, contour extraction algorithms can be applied (figure 1 (a) and (b)). Furthermore, as it has already been mentioned, landmarks consist in a useful widely adopted shape representation. Morphometrics landmarks can be biological process points located because of some biological background reason (see in figure 1 (c) landmarks referring to the table 1). In other cases, we can define singularity points, such as curvature maxima, as landmarks.

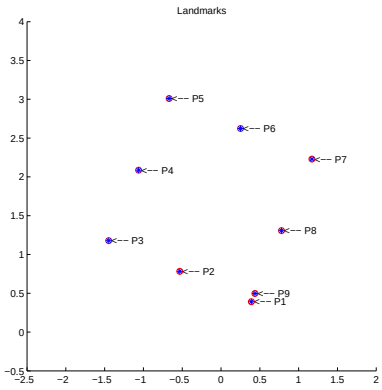

Figure 2. Landmark representation of a square.

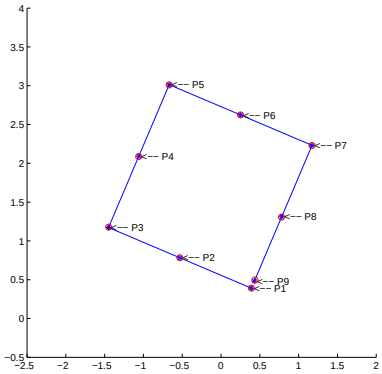

Figure 3. Interpolated landmarks of figure 2.

We follow the approach proposed in [1], in which the input to the wavelet transform is a complex signal representing the shape. Firstly, the landmarks are ordered so that, when two shapes are compared, the homologies between them are preserved (i.e. the landmarks from all shapes are ordered in a consistent manner, so that the i-th landmark of each shape is a homology w.r.t. the i-th landmark of all other considered shapes). The sequence of ordered landmarks can be viewed as the vertices of a polygonal line, being subsequently interpolated (linear interpolation, as shown in figure 1 (d)). This interpolation guarantees that the points along the polygonal line are uniformly spaced, which is fundamental in applying signal processing methods such as wavelets. A byproduct of this procedure is the fact that the total number of interpolated points can be chosen to be power of 2, thus allowing the application of efficient (i.e., $nlog(n)$) FFT algorithms to calculate the wavelet transform. It is worth noting that, in order to have a periodic signal that minimizes the wavelets border effects, it is important that the first landmark to be near to the last (not the same), what can be done by the interpolation procedure.

Thus, a landmark set l is interpolated generating a set of points (i.e. the polygonal line) denoted as $u(t) = (x(t), y(t))$. Therefore, the signal $u(t)$ can be defined as in equation 1 and applied as input for wavelet transform, as shown in the next section.

$$u(t) = x(t) + jy(t) \tag{1}$$

3 POLYGONAL WAVELET TRANSFORM

Wavelet transforms are mathematical tools for signal processing that can be applied in shape analysis [9]. They emphasize how the frequential content of the signal changes with time, considering that higher frequencies occur in short intervals while low frequencies spread in larger intervals. Let $u(t)$ be the complex signal representation obtained from the landmarks as explained in previous section. The continuous wavelet transform of $u(t)$ is defined as

$$U[\psi, u](b, a) = U_\psi(b, a) = \frac{1}{\sqrt{a}} \int_{-\infty}^{\infty} \psi^*(\frac{t-b}{a}) u(t) dt \tag{2}$$

$$U_\psi(b, a) = \sqrt{a} \int_{-\infty}^{\infty} \psi^*(af) U(f) e^{j2\pi fb} df \tag{3}$$

where $U_\psi(a, b)$ is the wavelet transform of $u(t)$, $a > 0$ is the scale parameter and b is the shift parameter of the mother wavelet ψ.

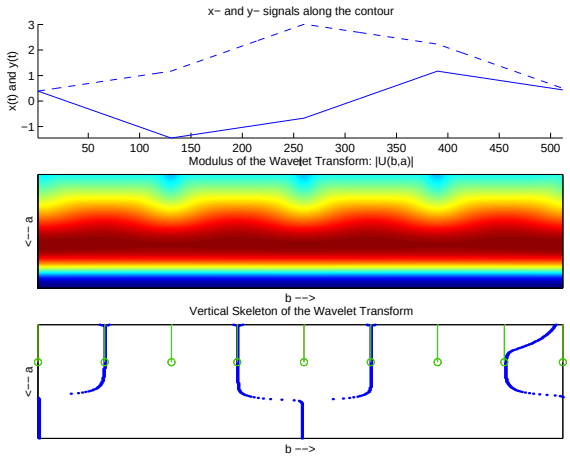

Figure 4. Wavelet transform with first gaussian derivative mother wavelet applied in the signal of figure 3.

In case the signal $u(t)$ is constructed to represent a shape contour, this transform is called W-representation [1]. This shape analysis tool has been successfully applied to different objects, including

for morphological classification of neural cells [9]. In this work, we show how it can be explored for analyzing the landmarks data, and, once the signal $u(t)$ represents a polygonal line, the obtained representation is called *polygonal wavelet transform*. The following section presents detailed analysis of the gaussian wavelet geometrical properties.

3.1 Gaussian Wavelet Transform Interpretation

It is remarkable the importance of differentiation operators in the context of signal analysis. For example, the tangent vector and the curvature, two of the main aspects regarding 2D shapes, are based on curve differentiation, allowing the identification of other shape features as inflection points, convex and concave corners, different measures of complexity. The differentiation property of the *Fourier* transform, together with the convolution theorem, allows applying the wavelet transform with n-th derivative-of-gaussian mother wavelet as an approximation of n-th derivative of $u(t)$. This fact was explored by A. Grossman in his classical paper [11]. These are some of the many advantages of calculating the derivative of signals using wavelets, thus explaining the interest of performing shape analysis using the derivatives-of-gaussian mother wavelet (like the Mexican hat, i.e. the second derivative of the gaussian).

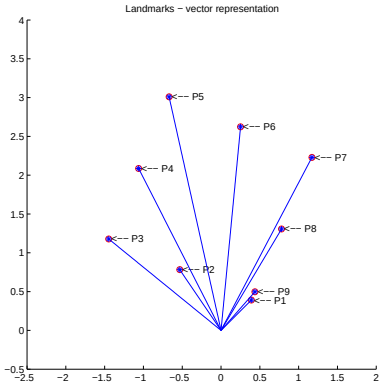

Figure 5. Vector representation corresponding to figure 2.

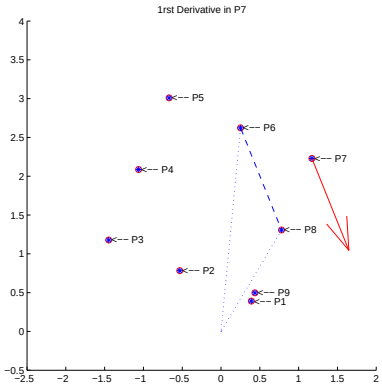

Figure 6. First derivative of the signal of figure 3 in P7, estimated by finite differences.

Furthermore, by taking the finite differences method as an approximation of the derivatives for the discrete case, this kind of wavelet

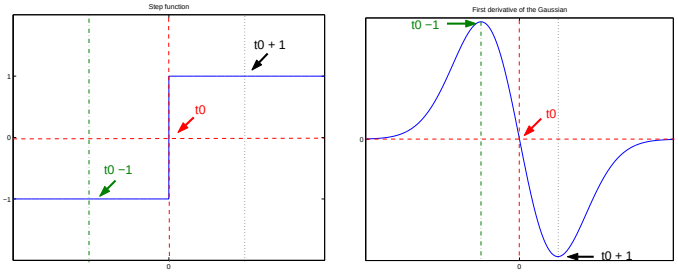

(a) (b)

Figure 7. (a) $[-1\ 0\ 1]$ differentiation mother wavelet; (b)First derivative of the gaussian mother wavelet.

transforms may be taken as a linear combination of vectors. The landmark representation of an object can be viewed as a set of vectors located at the system origin (see figure 5). Using this representation, it is possible to approximate tangent vector of the interpoled signal in each point using the wavelet transform. Therefore, let $u(t) = x(t) + jy(t)$ be a signal representing some polygonal line. For each t_0, $(x(t_0), y(t_0))$ defines a vector centered at the origin (i.e. $(0, 0)$) and pointing to $(x(t_0), y(t_0))$ (figure 5). Thus, we can estimate the tangent vector of $u(t)$ at t_0 as the vector difference $\vec{v'}_{t_0} = \vec{v}_{t_0+1} - \vec{v}_{t_0-1}$. For example, in figure 6 the tangent vector of the signal at P7 is calculated by difference between the vectors defined by P8 and P6 points, respectively.

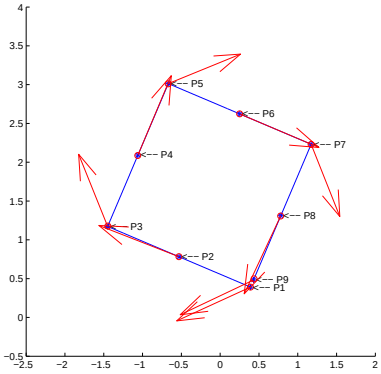

Figure 8. First derivative of the signal of figure 3, estimated by wavelet transform with first gaussian derivative mother wavelet (figure 4.

Observe that $\vec{v'}_{t_0}$ can be equivalently defined as $\vec{v'}_{t_0} = \psi(t_0 - 1)u(t_0 - 1)) + (\psi(t_0)u(t_0)) + (\psi(t_0 + 1)u(t_0 + 1)$, for $\psi(t_0 - 1) = -1$, $\psi(t_0) = 0$ and $\psi(t_0 + 1) = +1$, denoted as $[-1\ 0\ 1]$. This is locally equivalent to an inner product between ψ and u around (t_0). This idea can be generalized by taking ψ as a wavelet and, in the case of the first derivative-of-gaussian, a smoothed version of $[-1\ 0\ 1]$ (see figure 7 (a) and (b)). The wavelet transform using the second derivative-of-gaussian can also be geometrically interpreted using vectors in an analogous way.

4 RESULTS

The polygonal wavelet transform has been applied in the classification of real cases brain data in order to evaluate its effectiveness as a

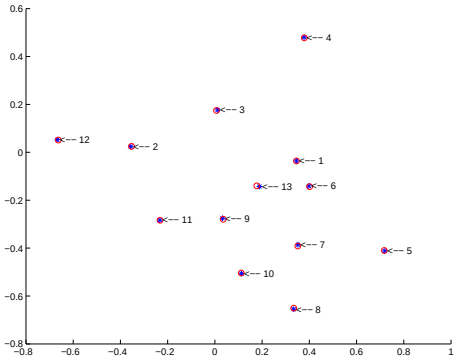

Figure 9. Landmarks

landmarks-based shape descriptor. We have used a data set composed by 13 anatomical landmarks for 28 parasagittal brain images (table 2). Among the considered training samples, fourteen cases were diagnosed schizophrenic and other fourteen are considered healthy. [3]

Table 2. Schizophrenia diagnosis landmarks

1	splenium, posteriormost point on corpus callosum
2	genu,anteriormost point on corpus callosum
3	top of corpus callosum, uppermost point on arch of callosum (all three to an approximate registration on the diameter of the callosum)
4	top of head, a point relaxed from a standard landmark along the apparent margin of the dura
5	tentorium of cerebellum at dura
6	top of cerebellum
7	tip of fourth ventricle
8	bottom of cerebellum
9	top of pons, anterior margin
10	bottom of pons, anterior margin
11	optic chiasm
12	frontal pole, extension of a line from 1 through 2 until it intersects the dura
13	superior colliculus

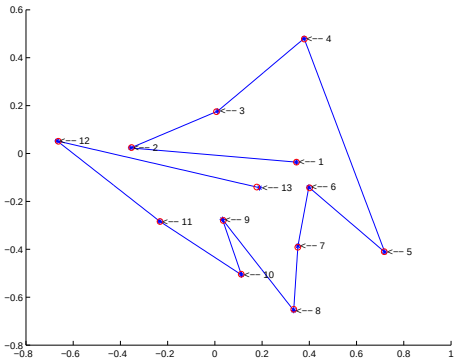

Figure 10. Interpoled landmarks of figure 9.

The previously introduced signal extraction methodology has been then applied to this set of landmarks, as illustrated in figures 9 and 10. These signals have been used as input to the polygonal wavelet transform using the first derivative-of-gaussian mother wavelet, as shown in figure 11). The training set has been then classified by a clustering algorithm known as linkage [9]. The clustering procedure requires the definition of a distance between the samples, which has been done using the wavelets point to point absolute difference. Let two shapes from the training set be represented by the complex signals $k(t)$ and $l(t)$. Let $K_\psi(a,b)$ and $L_\psi(a,b)$ be the wavelet transform of $k(t)$ and $l(t)$ respectively. Then, the distance between $k(t)$ and $l(t)$, denoted as $d(k,l)$, is defined as:

$$d(k,l) = m(|K_\psi(a,b) - L_\psi(a,b)|) \tag{4}$$

where $m(D)$ is the mean value of the matrix D.

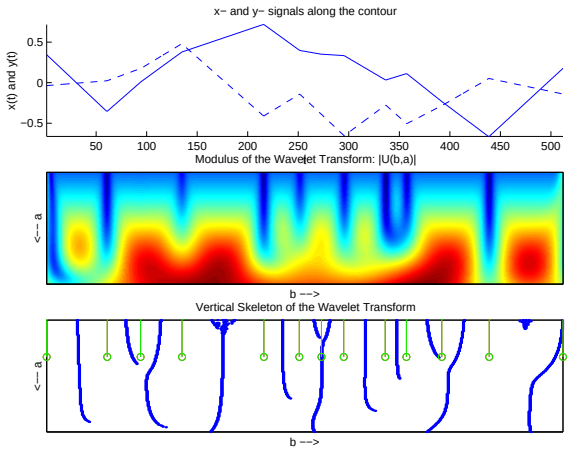

Figure 11. Wavelet transform with first derivative mother wavelet corresponding to signal of figure 10.

Observe that the initial data was divided between diagnosised schizophrenic cases labeled $\{6, 7, 8, 9, 10, 12, 13, 14, 15, 16, 17, 18, 19, 20\}$ and normal cases labeled $\{1, 2, 3, 4, 5, 11, 21, 22, 23, 24, 25, 26, 27, 28\}$.

The output of the linkage algorithm can be represented as a dendrogram, as shown in figure 12, thus emphasizing the similarity between the samples subsets. The dendrogram shows the schizophrenic and normal cases labels indicated above. The classification algorithm has grouped, as schizophrenic cases, the first 13 samples (from left to right) as shown in the dendrogram of figure 12. The correct recognition rate for the schizophrenic class is $84,6\%$, while for the normal class is 80%. Finally, additional experiments using both synthetic and real data have been perfomad producing equally encouraging results.

5 CONCLUDING REMARKS

This paper has presented a new approach for landmarks-based shape analysis using the wavelet transform. The proposed technique has been successfully applied to real data and the corresponding results have been shown. It should be mentioned that, although the approach discussed here concentrated on the 2D case, it can be straightforwardly generalized to 3D data, just requiring the formation of a 3D polygonal line joining the landmarks in some a priori defined order. In this case, a complex signal would not be used (in the sense of the 2D case where $u(t) = x(t) + jy(t)$. Instead, three distinct real signals $x(t)$, $y(t)$ and $z(t)$ should undergo the wavelet transform and be

[3] This data set can be found in the public morphometrics database at http://life.bio.sunysb.edu/morph/datasets.html.

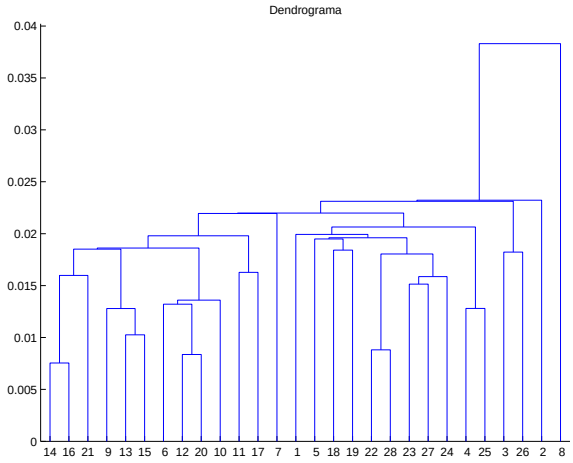

Figure 12. Classification with distance parameter as wavelets point to point difference.

used to form a 3D array of coefficients that could be used as features for a classification algorithm (e.g. the aforementioned linkage). It is worth mentioning that the proposed approach generalizes the capabilities for wavelet-based shape analysis, in the sense that it could be applied to *any* object represented by landmarks, not just contour-based shapes, which are limited to connected components. Exploring such 3D and other objects for classification are among our ongoing projects in developing the proposed techniques.

ACKNOWLEDGEMENTS

The authors are grateful to Marcel Brun for useful discussions. Roberto M. Cesar Jr. is grateful to FAPESP (99/12765-2) and to CNPq (300722/98-2 and 468413/00-6). Celina M. Takemura is grateful to CAPES.

We are grateful to the NEODAT project [4] for the figure 1 (a) (also http://research.amnh.org/ichthyology/neolit/neolit.html).Finally, we would like to thank F. Bookstein for make available the data set used for test in section 4 and to Sérgio R. Furtado for useful discussions on morphometrics.

REFERENCES

[1] J. P. Antoine, D. Barache, R. M. CesarJr., and L. F. Costa, 'Shape characterization with the wavelet transform', *Signal Processing*, **62**(3), 265–290, (1997).

[2] A. Arneodo, F. Argoul, E. Bacry, J. Elezgaray, and J.-F. Muzy, *Ondelettes, Multifractales et Turbulences: de l'ADN aux Croissances Cristallines*, Diderot Editeur, Arts et Sciences, Paris, 1995 (in French).

[3] A. Bimbo, *Visual information retrieval*, Morgan Kaufmann Publishers, San Francisco, California, 1999.

[4] F.L. Bookstein, *The measurement of biological shape and shape change*, Springer–Verlag, New York, 1978.

[5] F.L. Bookstein, *Morphometric tools for landmark data: geometry and biology*, Cambridge University Press, Cambridge, 1992.

[6] F.L. Bookstein and et al, *Morphometric in evolutionary biology*, Academy of Natural Sciences of Philadelphia, 1985.

[7] K.R. Castleman, *Digital image processing*, 303–347, Chapter 14: Wavelet Transforms, Prentice-Hall, Englewood Cliffs, 1996.

[8] M.J. Cavalcanti and et al, 'Landmark-based morphometric analysis in selected specis of serranid fishes(perciformes: Teleostei)', *Zoological Studies*, **38**(3), 287–294, (1999).

[4] For more information about NEODAT project see http://www.neodat.org/

[9] L.F. Costa and R.M. Cesar Jr., *Shape analysis and classification: theory and practice*, CRC Press, Boca Raton, 2001.

[10] I.L. Dryden and K.V. Mardia, *Statistical shape analysis*, John Wiley, Chichester, 1998.

[11] A. Grossmann, 'Wavelet transforms and edge detection', in *Stochastic processes in physics and engineering*, eds., M. Hazewinkel S. Albeverio, Ph. Blanchard and L. Streit (Eds.), Dordrecht, (1988). Reidel Publishing Company.

[12] P. E. Lestrel(ed.), *Fourier Descriptors and Their Applications in Biology*, Cambridge University Press, 1997.

[13] M. Leyton, 'A process-grammar for shape', *Artificial Intelligence*, **34**, 213–247, (1988).

[14] S. Loncaric, 'A survey of shape analysis techniques', *Pattern Recognition*, **31**(8), 983–1001, (1998).

[15] J. Marcgrave, *História Natural do Brasil*, Museu Paulista, Imprensa Oficial do Estado, São Paulo, 1942. With reproduction of original title-page: Historia natvralis Brasiliae... Lvgdvn. Batavorvim, apud F. Hackium, et Amstelodam: apud L. Elzevirium, 1648.

[16] T. Pavlidis, 'Algorithms for shape analysis of contours and waveforms', *IEEE Transactions on Pattern Analysis and Machine Intelligence*, **PAMI-2**(4), 301–312, (1980).

[17] E. Persoon. and K.S. Fu, 'Shape discrimination using Fourier descriptors', *IEEE Transactions on Systems, Man and Cybernetics*, **SMC-7**(3), 170–179, (March 1977).

[18] S. F. dos Reis, L. C. Duarte, L. R. Monteiro, and F. J. Von Zuben, 'Variation in mandible shape in *thrichomys apereoides* (mamalia: Rodentia): geometric analysis of a complex morphological structure', *Syst. Biol*, **49**(3), 563–578, (2000).

[19] C. G. Small, *The statistical theory of shape*, Springer Verlag, 1996.

[20] D'A. W. Thompson, *On Growth and Form*, Dover, 1992.